



PCCP

**Physical, Chemical and Biological Enhancement in X-ray
Nanochemistry**

Journal:	<i>Physical Chemistry Chemical Physics</i>
Manuscript ID	CP-PER-05-2019-003024.R1
Article Type:	Perspective
Date Submitted by the Author:	28-Jun-2019
Complete List of Authors:	Guo, Ting; University of California, Davis, Chemistry

SCHOLARONE™
Manuscripts

Physical, Chemical and Biological Enhancement in X-ray Nanochemistry

Ting Guo

Department of Chemistry, University of California, Davis, CA 95616

Abstract

X-ray nanochemistry studies how to use nanomaterials and particularly how to create new nanomaterials to increase effects of X-rays such as chemical reactivity, damage to cells, tumor destruction, scintillation and more. The increase, also called enhancement, can be categorized into several groups, and the current categorization of enhancement follows a natural division of physical, chemical and biological enhancement based on how nanomaterials behave under X-ray irradiation. In physical enhancement, electrons released from atoms in the nanomaterials upon X-ray ionization interact with the nanomaterials and surrounding media to increase the effects. Scintillation also belongs to this category. Chemical enhancement results when reactive oxygen species (ROS) or reactive radical intermediates (RRI) produced in aqueous solutions under X-ray irradiation interact with the surface of catalytic nanomaterials to increase the effects. When the damage of cells is enhanced through biological pathways beyond the abovementioned physical or chemical enhancement due to the presence of nanomaterials under X-ray irradiation, the enhancement is called biological enhancement. Works supporting this systematic categorization, the reported values of these enhancements, and important aspects of the development of enhancement in the X-ray nanochemistry framework are given and discussed in this perspective.

1. Introduction

X-ray nanochemistry is a new discipline that studies how to create nanosystems to enhance the effectiveness of X-ray irradiation, which is equivalent to developing nanomaterials to increase the responses by solid-state, chemical or biological systems to X-ray irradiation.¹ The goal of X-ray nanochemistry is therefore to design and optimize nanosystems to respond to or harvest X-rays by converting X-ray energies to other forms of energy or actions. Since X-rays are still photons, X-ray nanochemistry can also be called X-ray photo-nanochemistry, highlighting strong connections to photochemistry. In this sense, nanosystems are analogs to traditional photosystems in photochemistry, with the biggest difference being that X-ray photons are much more energetic and highly penetrating, even in optically opaque materials. X-rays also have low diffraction limit, on the order of angstrom. The consequences are that absorption of X-rays is usually spread into larger volumes or over greater depths than UV-Vis photons and each absorption event produces many more ROS or RRI than each UV-Vis photon absorption event does. Therefore, X-rays can reach places UV-Vis photons cannot.

X-ray nanochemistry investigates how to build chemical, nanochemical or other systems to respond effectively to X-ray irradiation with nanometer spatial precision using X-ray or electron absorbing nanomaterials. In this regard, nanomaterials can generate enhancement by either directly absorbing more X-rays or catalyzing reactions of interest through interacting with reactive species including electrons produced by X-ray interactions with the surroundings which include solvents and other nanomaterials and additives. The latter mechanism also has nanometer spatial resolution because it relies on the surface of nanomaterials. These two mechanisms, direct and indirect, can exist independently or together and can be complementary to each other.

X-ray nanochemistry resembles but differ from photochemistry. Unlike photochemistry which can be modeled after photosystems in plant cells, it is not known that nature has provided much guidance to X-ray nanochemistry research. Prior to the development of X-ray nanochemistry, little knowledge exists on

how nature harvests X-rays. In biological systems, there are mechanisms such as DNA damage repair processes or programmed apoptosis that counter the effects of ionizing radiation. These repair systems, however, are most likely created to counter reactive species such as radicals or oxidants created by chemical processes, and not by purposeful or natural exposure to ionizing radiation.² Another important evidence for a lack of existing natural X-ray harvesting systems is that there are no known natural radiation sensitizers found in living systems, suggesting that nature does not or does not need to take advantage of X-rays or other ionizing radiation. This, however, does not mean that there is no advantage of utilizing ionizing radiation. If nanosystems can be created to respond to and harvest X-rays like plant cells respond to sunlight, then many new applications can be developed, possibly duplicating the story of how today's chip industry for personal phones, computers and other devices are developed based on the creation of semiconductor materials in the 1950s.

X-ray nanochemistry is still in its infancy and includes at least four main research areas, which are theoretical studies, syntheses of nanomaterials, methods to measure enhancements, and applications in many areas, including biology, cancer diagnosis and treatment, catalysis, environmental remediation, and sensing. The nanosystems used in X-ray nanochemistry to date are mostly simple nanoparticles. There are only a few cases in which the origins of enhancement are clearly understood. Nevertheless, various enhancement mechanisms have been proposed.¹ The focus of this monograph is on the description of three main categories of enhancement.

Enhancement is categorized as physical, chemical or biological, depending on the pathway by which it arises as explained in several reviews and a recent book.^{1, 3-5} Enhancement studies are thus at the core of X-ray nanochemistry research. Each category of enhancement is further divided into many types and each type may contain several kinds. The reason for categorizing and dividing the enhancement into types and kinds is that such divisions entail the nature of these enhancements and enable us to better understand how to achieve the highest total enhancements when individual enhancements are combined. These categorizations may expand and change over time, as the discipline evolves.

2. X-ray Nanochemistry and Enhancement: General Definition and Units

X-ray nanochemistry studies all aspects of the enhancement processes. The most commonly used figure of merit in the literature to describe the improved effectiveness is the dose enhancement factor, due largely to close connections of the early work performed in X-ray nanochemistry to cancer treatment. This term, however, is inadequate to describe all the important processes in X-ray nanochemistry because it is too generic and does not differentiate among various categories, types and kinds of enhancement. Consequently, the dose enhancement factor is replaced with physical, chemical or biological enhancement, and with even more refined terms such as type 1 physical enhancement (T1PE) or type 2 biological enhancement (T2BE).

The enhancement has a generic unit of dose enhancement units (DEU), similar to Hounsfield Units (HU) used to describe contrast in X-ray imaging. An important aspect of enhancement is whether it is relative or absolute. Relative enhancements are benchmarked against the magnitude of response to X-rays by the background materials such as water or solvents without nanomaterials. Therefore, a relative enhancement of 1.0 DEU means no enhancement. Absolute enhancements are relative enhancements minus 1.0. Consequently, a 1.0-DEU absolute enhancement, which is also benchmarked against the background response, is a 100% increase over the response by the sample sans nanomaterials. Unless specifically noted, absolute enhancements are used as the default enhancement here, even though relative enhancements are more widely used in the literature.

3. Categories, Types, and Kinds of Enhancements

There are at least three categories of enhancements: physical, chemical and biological. These enhancements are defined and discussed in this perspective. Figure 1 illustrates these three categories and the relationships among them. In this picture, physical enhancement (PE) is generated by a large nanoparticle made of heavy elements (labeled as NP-A) with an inert surface. An electron track (dark line) is shown, along with hydroxyl radicals (red dots) produced through electron-water interactions. Chemical enhancement (CE) is created by a small catalytic nanoparticle (NP-B), and biological enhancement (BE) is caused by an inert, low atomic number (Z) small nanoparticle (NP-C). In this illustration, a DNA strand break reaction between the strand and a hydroxyl radical is used as the target of enhancement. Repair of DNA strand breaks by repair proteins (a SUMO protein is shown here) is used as an example of BE, which shows that if its function is blocked by the nanoparticle, then the efficiency of DNA cleavage is increased. Each category can be further divided into several types, which will be discussed in the following. When all three enhancements are present, the total enhancement is a complex function of three enhancements.

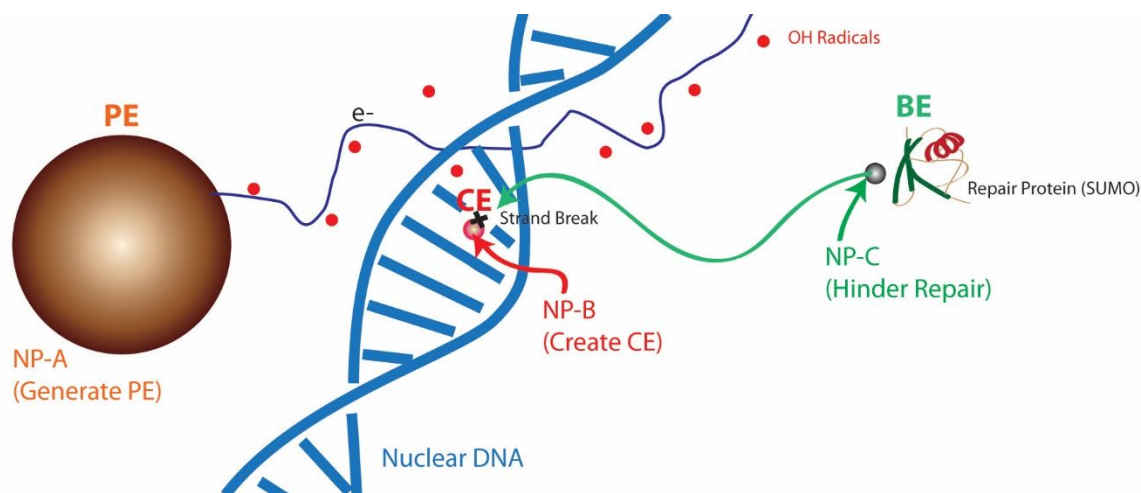


Figure 1. Illustration of and relationships among three categories of enhancement enabled by three different nanomaterials. A nuclear DNA segment (blue) is shown here as the chosen target of damage. OH radicals (red dots) produced by electrons released from NP-A can break the strand to generate physical enhancement (PE). Chemical enhancement (CE) occurs when NP-B interacts both catalytically and directly with the strand. Biological enhancement (BE) happens when NP-C interferes with the function of the repair proteins, therefore increasing the strand break efficiency. Without NP-C, damaged DNA strands would be repaired by the repairing proteins. A SUMO protein is shown as an example, and nanoparticle NP-C itself can, but does not need to be able to cause strand breaks or protein damage; NP-C just needs to be physically present at the repair protein location to hinder the repair function.

3.1. Physical Enhancement

3.1.1. Introduction: Physical Processes of Improving the Effectiveness of X-ray Induced Responses

Physical enhancement (PE) is the most precisely defined and broadly accepted enhancement category among the three categories of enhancement described here. PE causes enhanced effects of X-ray irradiation without any chemical or biological influences, meaning there are neither catalytic effects nor involvement of biological pathways. Another way to define PE is that the measured enhancement can be completely explained by the measured or predicted energy deposited in a target volume by the electrons released from nanomaterials as a result of X-ray absorption. The absolute enhancement of PE is the ratio of energy deposited in the medium with nanomaterials to that without nanomaterials.

PE can be best understood as described in Figure 2A. The enhancement process begins with X-ray absorption by nanomaterials (marked as Step 1), which leads to the emission of electrons (Step 2). For simplicity, only one electron and its track is shown. A typical energy spectrum of the electrons released from the gold nanoparticle is shown in Figure 2B. Depending on the X-ray energies and absorbing

elements, the energy of the electrons released from the nanomaterials changes from a few eV to tens of keV. These electrons then deposit energy in the surrounding medium (Step 3). The deposited energy is usually exhibited in the form of reactive oxygen species (ROS), which can be detected by reacting with probes such as coumarin 3-carboxylic acid (3-CCA) to form detectable products. Even without nanomaterials, the medium still absorbs X-rays through various processes such as the photoelectric effect, Compton scattering or pair production. The process of Compton electron production and interactions of Compton electrons with the medium are shown in Figure 2A as well, marked by Steps i, ii, and iii. The energy absorbed by the medium without nanomaterials represents the baseline or denominator in the ratio used to calculate the enhancement. In the presence of nanomaterials, there is an increased amount of energy deposition in the sample, which is the enhanced part that appears in the numerator of the ratio of the enhancement calculation as shown in the equation in Figure 2A. The enhancement is called PE if it is solely caused by the increased energy deposition by the nanomaterials.

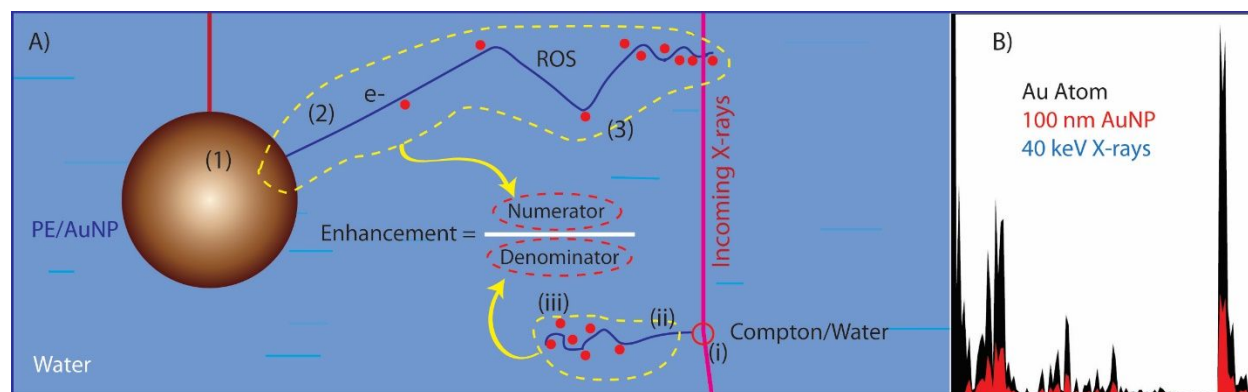


Figure 2. Origin of physical enhancement (PE). A) shows the processes of X-ray absorption (Step 1), electron emission (Step 2), and energy deposition (Step 3) associated with the absorption of X-rays by the nanoparticle, and similar steps i, ii, and iii associated with X-ray absorption by the medium are shown as well. The enhancement is calculated using the ratio of energy deposition in the medium with nanoparticles (numerator) to that of the medium itself (denominator). B) shows the electron spectrum from 40 keV X-rays irradiating gold atoms and 100-nm gold nanoparticles in water. Four peaks are shown, at 200, 500, 2000 and above 10000 eV.

The processes described here can also be considered an energy transfer process from X-rays to electrons and then to other forms of energy such as chemical energies. This energy transfer should be non-catalytic and without biological regulations. If the electrons interact with semiconductor nanomaterials, then the energy transfer process can possibly induce emission of UV-Vis photons.¹ PE is often measured using chemical or biological reactions, which can introduce nonlinear and complex responses. If this is the case, then these measurements make the detection susceptible to the influence of other categories of enhancement.

The types of PE can be defined by the way in which energy is transferred from X-rays through energy deposition by electrons to other forms of energy if there are no interferences from chemical, biological or other processes. Type 1 physical enhancement arises when the energy is uniformly deposited in the whole sample volume. Energy deposited only near the surface of the nanoparticles gives rise to type 2 physical enhancement. Type 3 physical enhancement occurs when energy is deposited in the nanomaterials and then transferred to UV-Vis photons. All three enhancement types are discussed in this section.

3.1.2 Type 1 Physical Enhancement

Type 1 physical enhancement (T1PE) exists in most enhancement studies, although it is not always straightforward to observe because T1PE may be negligible if the amounts of nanomaterials are too little or the measured enhancement contains or is even dominated by other categories of enhancement.

T1PE is caused by X-ray absorption by nanomaterials, and it is enabled by the electrons released from these nanomaterials traversing and depositing energy in the surroundings. T1PE specifically means that the increased energy deposition generated by these electrons is nearly constant over the entire sample volume.

Theoretical studies of T1PE are frequently reported in the literature, the first of which appears soon after the first report on enhanced tumor treatment of mice using gold nanoparticles.⁶ For gold in water, which is the most popular composition used in X-ray nanochemistry to demonstrate enhancement, calculations and measurements show that the magnitude of enhancement is approximately 1.0 DEU per 1 weight percentage (WP) of gold in water, which can be expressed as 1.0 DEU WP⁻¹ (Au/H₂O) or simply 1.0 DEU WP⁻¹.^{1,3} A number of theoretical works have been reported and the results are shown in Table 1.

Table 1. List of theoretical studies of T1PE. Only exclusive T1PE studies are shown here. Adapted from reference ¹.

Element	Size (nm)	X-ray Energy	Enhancement	Unit mass enhancement	References
Au	2, 50, 100	50 kVp, 250 kVp, 60Co, 6 MV	10-2000 ^{a)}	--	7
Au	2-50	20-150 keV	0.06 ^{b)}	1.2	8
Au	88	100 kVp	Up to 7.0	1.0	9
Au	70	100 kVp	0.7	0.7	10
Au	30, 50	1170 keV, 6 MV	0.5-2.95 ^{c)}	--	11
Au, Pt	100,000	380 keV	0.15-0.3 ^{b)}		12
Z=14-80	20	1 keV-10 MeV	<0.3	6.0 ^{b)}	13

a) single nanoparticle irradiation configuration. b) physical enhancement. c) wire configuration.

Even though many theoretical works have reported T1PE, experimental measurements of exclusive T1PE are scarce. It is difficult to measure only T1PE because there are often other enhancements that also contribute to the measured total enhancement, which complicates the identification and isolation of T1PE from those categories or types of enhancement. The only experimental account of pure T1PE reported in the literature is achieved through using large gold nanoparticles coated with an inert silica layer to remove other categories and types of enhancement.⁹ The large gold nanoparticles support T1PE while the silica coating reduces type 2 physical enhancement to minimal and simultaneously eliminates chemical enhancement. No biological enhancement existed in their measurements. Figure 3 shows the nanomaterials (Figure 3A) and the representative results (Figure 3B). The slope of the enhancement per unit mass is 1.0 DEU WP⁻¹ using the data at low gold concentrations. This result agrees with the magnitude of the theoretically predicted T1PE shown in Table 1.

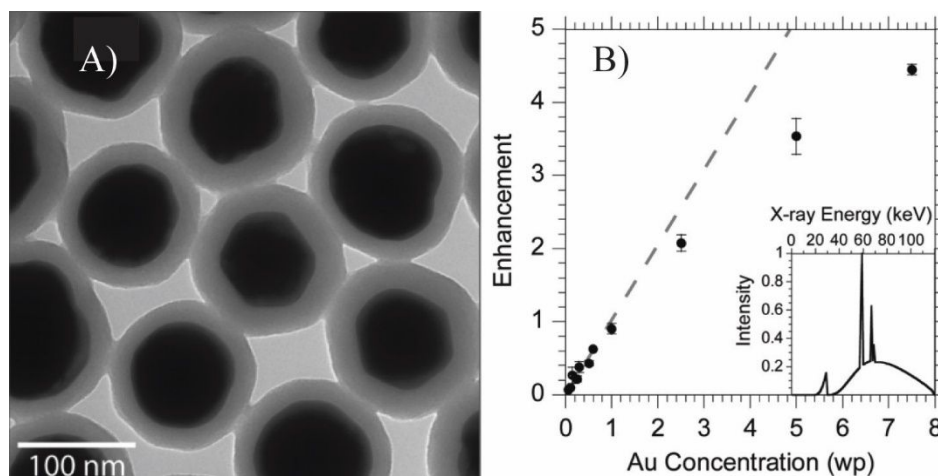


Figure 3. Experimentally determined exclusive type 1 physical enhancement (T1PE). A) shows the silica-covered gold nanoparticles and B) presents the measured T1PE as a function of the gold concentration in the units of weight percentage (WP) of gold in water. The enhancement is expressed in absolute enhancements. The slope is the unit mass enhancement, which is 1.0 DUE WP^{-1} obtained using data at low gold concentrations. At higher gold concentrations, the slope decreases due to energy deposition in gold.⁹

As will be made clear in the next section, when only types 1 and 2 physical enhancement exist and if the probes are uniformly distributed over the whole volume, which is often the case, then the total enhancement is dominated by T1PE, especially for large nanoparticles – over 70% of the total enhancement is T1PE for 100 nm nanoparticles if there is no chemical enhancement or scavenging. This straightforward guideline represents the main benefit of identifying T1PE. Unfortunately, these conditions are not often satisfied. For instance, anti-enhancement can be strong when T1PE is strong. As a result, measured enhancements often deviate from the predicted T1PE when other enhancements such as type 1 chemical enhancement or anti-enhancement dominates.

3.1.3. Type 2 Physical Enhancement

Type 2 physical enhancement (T2PE) exists predominantly near the surface of nanomaterials. It is caused by electrons, and particularly low-energy electrons, depositing energy near the surface of the X-ray absorbing nanomaterials. The profile of such deposition depends on the size and shape of nanomaterials. Small nanoparticles have their T2PE within a few nanometers of the surface of nanoparticles, and the magnitude of the peak intensity of T2PE, which is close to the surface, for these small nanoparticles is low.¹⁴⁻¹⁵ For large nanoparticles, the magnitude of the peak enhancement is significantly higher than small nanoparticles. The full width at half maximum (FWHM) of the T2PE profile as shown in Figure 4A is typically 20-50% of the nanoparticle diameter. T2PE has been explored and cited using different terms such as nanoscale energy deposition or nanoscale dose effect.¹⁴⁻¹⁶ The detection of T2PE itself is difficult if the probes are uniformly distributed over the whole sample volume (Figure 4A). The measured enhancement is the sum of T1PE and T2PE and is often dominated by T1PE. Near the nanoparticle surface, both types of enhancement exist, but T2PE is usually much stronger. Consequently, when the probes are placed only near the surface, T2PE can be sensitively and nearly exclusively measured, as shown Figure 4B.

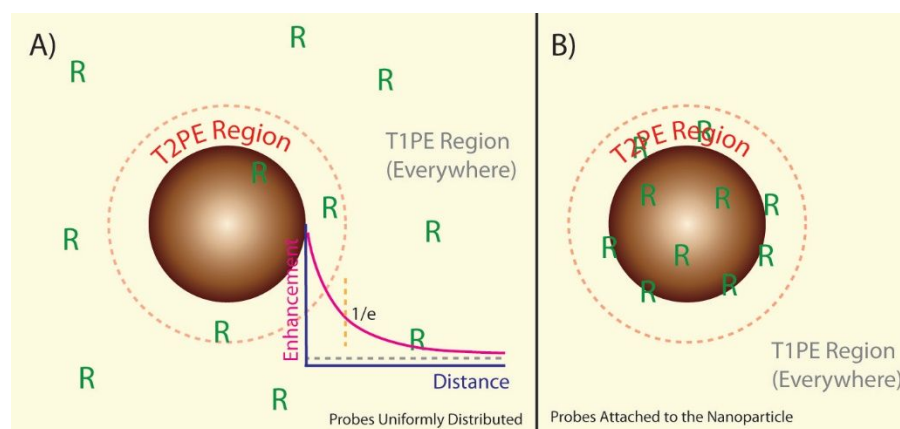


Figure 4. Type 2 physical enhancement (T2PE) around a nanoparticle. A) displays a large nanoparticle with T2PE around it while T1PE occupies the entire sample volume. Probing reactions (R) are uniformly distributed in the entire volume. B) shows the probes conjugated to the surface of the nanoparticle. T2PE is more exclusively measured in this configuration.

Theoretical and experimental studies of T2PE have been reported in the literature and some of them are listed in Table 2. T2PE is best understood and studied with theory because the spatial profile and magnitude of the enhancement are revealed. The enhancement profile follows the electron energy deposition profiles and can be precisely simulated. Two parameters, the FWHM for the enhancement profile and peak enhancement values at the surface, are retrieved from the literature reports and listed in Table 2. The units of enhancement are DEU and absolute enhancements are expressed. 3-nm gold nanoparticles have the lowest peak enhancement of nearly 3.0 DEU and the shortest FWHM of 1 nm.¹⁴ For large, 100-nm diameter gold nanoparticles, peak T2PE within a 1-nm shell off the surface is 14 DEU and the FWHM is approximately 22 nm for X-rays from 14 keV to 100 keV. These results are shown in Table 2.

Table 2. List of work for type 2 physical enhancement studies. Adopted from reference ¹.

Element	Size (nm)	Energy	Peak Enhancement (DEU)	FWHM (nm)	Ref.
Au	3	100 kVp	0.6	~1	14
Au	90	100 kVp	2.0	20	17
Au	Atoms	50 kVp, 6MV, ¹²⁵ I, ¹⁰³ Pd, ¹⁶⁹ Yb, ¹⁹² Ir	10-1000*	~250	18
Au	2, 50, 100	50, 250 kVp, ⁶⁰ Co, 6 MV	10-2000*	>1500	7
Au	500	100 kVp	9	~200	19
Au, Pt, Bi	1000	50 kVp	7.2	~250	20
Au	100 nm slab	50 keV	11-42	~50	21
Au	~30 mm	35-95 keV	17.5	~2 mm	22

* Nanoscale X-ray beam profile irradiation.

Experimentally, careful designs are required to measure T2PE. In a recent report, T2PE is measured without the influence from chemical or anti-enhancement.²³ The design and results are shown in Figure 5. The detection of enhancement employs strand breaks of single strand DNA linking green fluorescence proteins (GFP) to the surface of silica-coated gold nanoparticles.²³ The label “1N-GFP” indicates that the GFP are modified so that there is approximately only one DNA linker between each GFP and the anchoring nanoparticles, as shown in Figure 5A (bottom). “XN-GFP” signifies multiple DNA linkers between a GFP and the anchoring nanoparticles. DNA strand breaks at the surface of silica-coated gold nanoparticles are used to measure T2PE, which is close to the configuration described in Figure 4B. The silica layer, necessary to block chemical enhancement and anti-enhancement, reduces the magnitude of

T2PE from 14 DEU to 10 DEU, as revealed by theoretical simulations. Figure 5B shows the experimental results. The magnitude of the enhancement is calculated using the ratios of DNA strand break efficiencies measured with AuNP@SiO₂ to SiO₂NPs. The strand break efficiency is equivalent to the GFP release efficiency shown in Figure 5B. The enhancement is 36 DEU, greater than the theoretically predicted value, possibly because the results are influenced by a combination of T2PE, number and diffusion of OH radicals near the DNA strands and the solid angle of OH radicals reacting with the DNA on the surface through collisions. The measured strand break efficiency is lower for GFP on bare AuNPs, possibly due to scavenging of hydroxyl radicals by the gold surface.

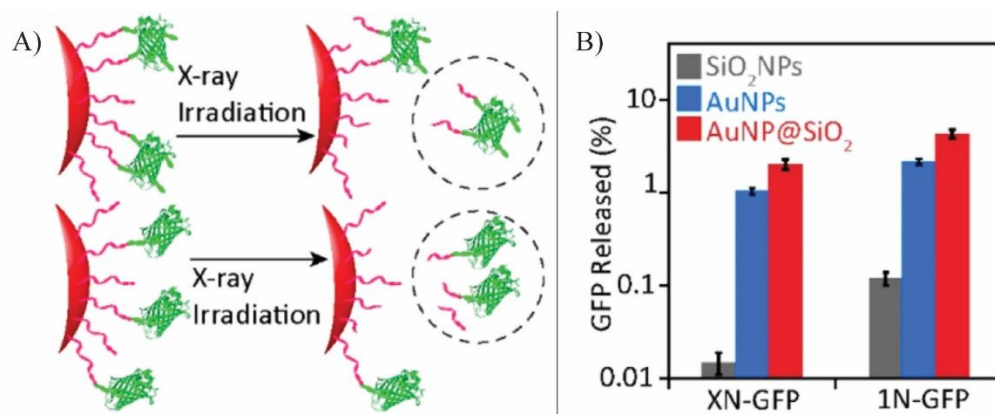


Figure 5. An example of Type 2 physical enhancement (T2PE) measurements. A) displays the green fluorescence proteins (GFP) linked to the surface of nanoparticles (red spherical cap) through a single 12-mer DNA strand (red line). Upon X-ray irradiation, the DNA strands are cleaved and GFP are released. GFP fluorescence is detected using fluorimetry to determine the enhancement. B) shows the results of the measurements, and a 36-DEU enhancement (the ratio of GFP released from AuNP@SiO₂ (red bar) to SiO₂NPs (grey bar)) is seen for 100 nm gold nanoparticles covered with a layer of silica.²³

A special case of T2PE is X-ray induced energy transfer (XIET), which is illustrated in Figure 6.²⁴ This type of energy transfer derives from electrons released from X-ray absorbing nanomaterials depositing energy in nearby nanomaterials. The X-ray absorbing, electron emitting nanomaterial is called the donor, and the electron receiving nanomaterial is called the acceptor. The absolute efficiency of XIET between two nanoparticles shown in Figure 6 is low, on the order of 1% because only a small fraction of the X-ray photon energy is deposited in the acceptor. For example, for a 100 nm diameter gold nanoparticle donor next to a water-filled silica shell acceptor of a 100 nm outer diameter and a 10-nm shell thickness, the amount of energy deposited in the acceptor by the electrons released from the gold nanoparticle donor is 7.4 eV when the sample is irradiated with 14 keV X-rays at 1 Gy dose. These electrons deposit approximately 560 eV in a 10- μ m water cube surrounding the acceptor. This means the absolute XIET efficiency, which is the amount of energy deposited in the acceptor divided by that in the rest of the sample, is 1.3%, far less than the near 100% Förster Resonance Energy Transfer (FRET) efficiency in the optical regime.²⁵ The X-ray dose or flux needed to cause a single 14-keV X-ray photon absorption per 100 nm gold nanoparticle is approximately 25 Gy. At this dose, the 1.3% XIET efficiency means that for a single X-ray absorption of a 14-keV X-ray photon by a 100-nm gold nanoparticle, the amount of energy deposition in the acceptor is 182 eV, much higher than the amount of energy (~2.5 eV) transferred from a donor to an acceptor through FRET as a result of absorption of a single visible photon. XIET efficiency can also be expressed in PE. In this case, the amount of energy deposited in the shell by X-rays is 3.1 eV without the nanoparticle donor at 1 Gy irradiation, resulting in a $(7.4/3.1-1.00)=1.39$ DEU absolute enhancement (right panel, Figure 6).

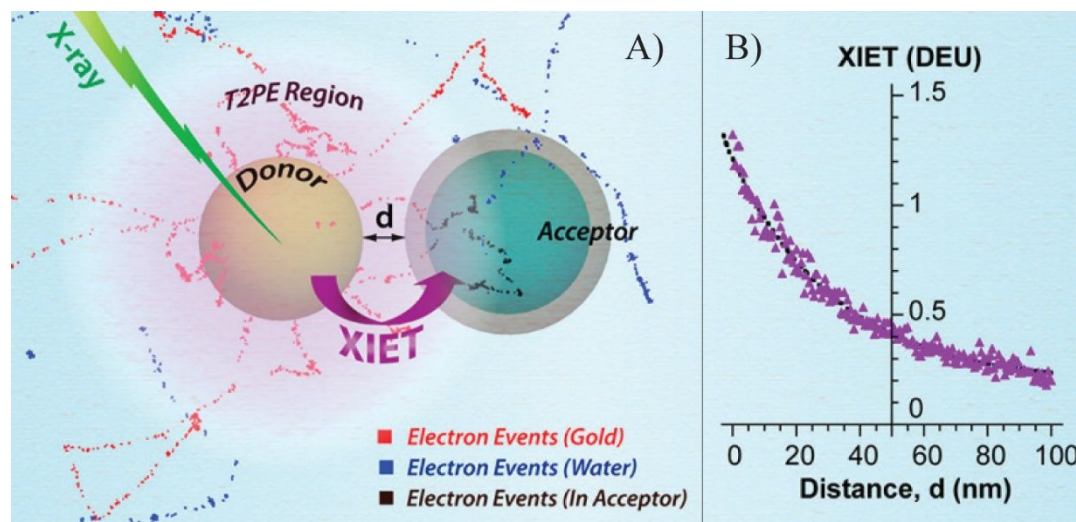


Figure 6. Illustration of XIET. A) describes the XIET process, starting with X-ray absorption by the donor. XIET magnitude depends on the distance between the donor and acceptor d . For the acceptor in the T2PE region, XIET is strong enough to be detected. B) shows the calculated distance dependency results for relative XIET efficiency in terms of PE.²⁴

3.1.4. Type 3 Physical Enhancement

Type 3 physical enhancement (T3PE) is manifested in X-ray generated UV-Vis photons. A similar process is described in a recent report (p 99).¹ Typically speaking, in T3PE X-rays induce the emission of visible photons in semiconductor or rare earth nanomaterials. It is also possible to use processes such as FRET to induce T3PE. These direct and indirect energy transfer processes create at least two kinds of T3PE, which are illustrated in Figure 7. If the nanomaterials per unit volume directly absorb more X-rays than the surrounding (Figure 7A) and the increased absorption directly leads to the production of more electron-hole pairs and/or more scintillation photons, then this is the first kind of type 3 PE noted as T3PE(1). This kind of T3PE is the most commonly encountered T3PE.²⁶ The nanomaterials responsible for T2PE(1) are made of scintillation materials of heavy elements (Figure 7A), making the nanomaterials absorb X-rays intensely and capable of generating types 1 and 2 physical enhancement. In one publication, the absolute conversion efficiency of X-rays to UV-Vis photons is measured at 6% using Eu:Gd₂O₃ nanoparticles.²⁷ This efficiency is higher than the absolute XIET efficiencies mentioned earlier. If the introduced nanomaterials are made of lower atomic number elements (e.g., silicon) which absorb less X-rays than the surrounding media such as bromoform, then electron-hole pairs in the nanomaterials are more likely excited by electrons produced from the X-ray absorbing surrounding media and not the nanoparticles themselves. The resulting enhancement is the second kind of T3PE or T3PE(2) (Figure 7B). Silicon nanoparticles, being a scintillation material and emitting at around 425 nm, suspended in water or in cells can cause T3PE(2).²⁸

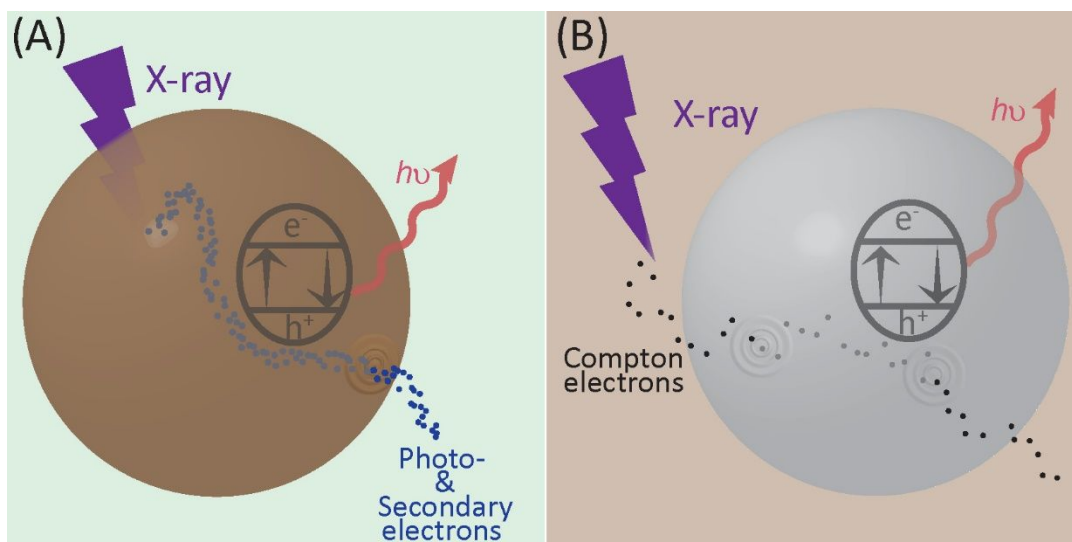


Figure 7. Illustration of type 3 (scintillation) physical enhancement (T3PE). A) show the first kind T3PE, T3PE(1), which is most common. In this process, X-rays are absorbed by the nanomaterials, and electrons are released from the absorption site/atom. These electrons then excite the semiconductor nanomaterial to produce UV-Vis photons. B) displays the second kind of T3PE, T3PE(2), in which the nanomaterial itself does not intensely absorb X-rays; instead it interacts with electrons produced from X-rays interacting with the surrounding medium to produce UV-Vis photons.

3.1.5. Applications of Physical Enhancement

PE has been the intended enhancement in many applications, although the nanomaterials employed in these applications may also support other categories of enhancement. With the assistance of theoretical simulations, it is now possible to predict the magnitude of at least two types of PE when the amount and location of nanomaterials used in these applications are known, though such information may not always be available to researchers. These potential applications can be supported by inexpensive desktop microfocus X-rays or even palm size X-ray sources. Among the three types of PE, T2PE may have the greatest potential because of the high magnitude of enhancement associated with T2PE. As a result, it is possible to use large nanoparticles to generate T2PE near the surface of nanoparticles, a process that can be used in many applications. T3PE may also play an important role in many applications, although it is often difficult to differentiate it from T2PE.

3.2. Chemical Enhancement

Chemical enhancement (CE) is defined as the enhanced X-ray effects caused by the chemical properties of the nanomaterials. The most common process that causes CE is catalysis. As it is shown below, CE does not require the nanomaterials to absorb X-rays.

3.2.1. History and Introduction

CE is different from PE. When CE dominates, the magnitude of increase to chemical reactivity of interest usually far exceeds the increased amount of absorption of X-rays by the added nanomaterials. For example, the increase of a chemical reaction yield over the entire sample volume can reach 300%, whereas the increase of X-ray absorption by this nanomaterial is merely 1%. In such cases the increased absorption cannot explain the enhanced yield. If the yield is measured locally, i.e., around the surface of nanomaterials, then a validation must be provided by examining whether the yield increase is greater than the predicted T2PE or not. If it is, then the measured enhancement must not originate from T2PE either.

There are at least two types of CE. If there is little change to ROS production and the yield of the reaction of interest increases because of the catalytic surface of the added nanomaterials, then this type

of CE is called type 1 chemical enhancement.²⁹ A second type of chemical enhancement has been implied in the literature. In this case, the nanomaterials are claimed to absorb X-rays to enable catalysis and the amount of ROS is claimed to be increased catalytically.³⁰ However, there has been no direct evidence to support that this type of enhancement is caused by the absorption of X-rays by the nanomaterials. This type of CE also includes another special enhancement, anti-enhancement, which has been observed by many groups.³¹⁻³⁴ In this special case the added nanomaterials such as gold nanoparticles scavenge rather than produce more ROS.

3.2.2. Type 1 Chemical Enhancement

Type 1 chemical enhancement (T1CE) is enabled by the surface of nanomaterials. As a result, the surface should be catalytically active towards the reactions of interest. Another requirement is that ROS production should not change when nanomaterials are added. There are several reports in the literature that support the existence of T1CE.

In one example, electron parametric resonance (EPR) spectroscopy and 3,4-dihydro-2-methyl-1,1-dimethylethyl ester-2H-pyrrole-2-carboxylic acid-1-oxide (BMPO) spin trapping agent are used to study the enhancement by gold nanoparticles (AuNPs).³⁵ The nanoparticles are sub-five nanometer AuNPs covered with Tetrakis(hydroxymethyl)phosphonium chloride (THPC) ligands. BMPO reacts with hydroxyl radicals ($\bullet\text{OH}$) to form the $\bullet\text{BMPO-OH}$ spin adduct that has a lifetime of 40 min. When BMPO aqueous solutions are irradiated with X-rays in the presence of AuNPs, $\bullet\text{BMPO-OH}$ is found to be converted to $\bullet\text{BMPO-H}$. The long-lived $\bullet\text{BMPO-OH}$ intermediate allows the separation of $\bullet\text{OH}$ production step from catalytic conversion of $\bullet\text{BMPO-OH}$ to $\bullet\text{BMPO-H}$. The experimental results show that AuNPs indeed catalyze the conversion of $\bullet\text{BMPO-OH}$ to $\bullet\text{BMPO-H}$ by spiking the irradiated BMPO aqueous solutions with AuNP solutions. The rate constants are retrieved, and ROS production is found to be slightly reduced by the THPC-AuNPs. The EPR patterns of the signals without and with THPC-AuNPs are shown in Figure 8A. If the left most peaks of $\bullet\text{BMPO-H}$ EPR patterns are used to calculate the enhancement, then adding AuNPs causes a 1.4 DEU enhancement. Nearly identical EPR results are obtained when either the BMPO solution is irradiated and then spiked with THPC-AuNPs, or when the mixture of BMPO and AuNP solutions is irradiated, proving the enhancement is caused by AuNPs catalyzing the conversion from $\bullet\text{BMPO-OH}$ to $\bullet\text{BMPO-H}$. A triple jump analogy is invoked to help elucidate the process. The sports model shows that the total distance is a combination of three individual phases, and an increase of the overall distance does not always mean the increase of the distance cleared by the first phase (Figure 8B). This analogy shows that the increased $\bullet\text{BMPO-H}$ yield does not necessarily mean the increased production of $\bullet\text{OH}$, which belongs to the first phase. In this example, only the third phase is catalyzed. The second phase is not affected due to the high concentration (25 mM) of BMPO employed in the experiment, which is much higher than that of THPC-AuNPs (<500 nM).

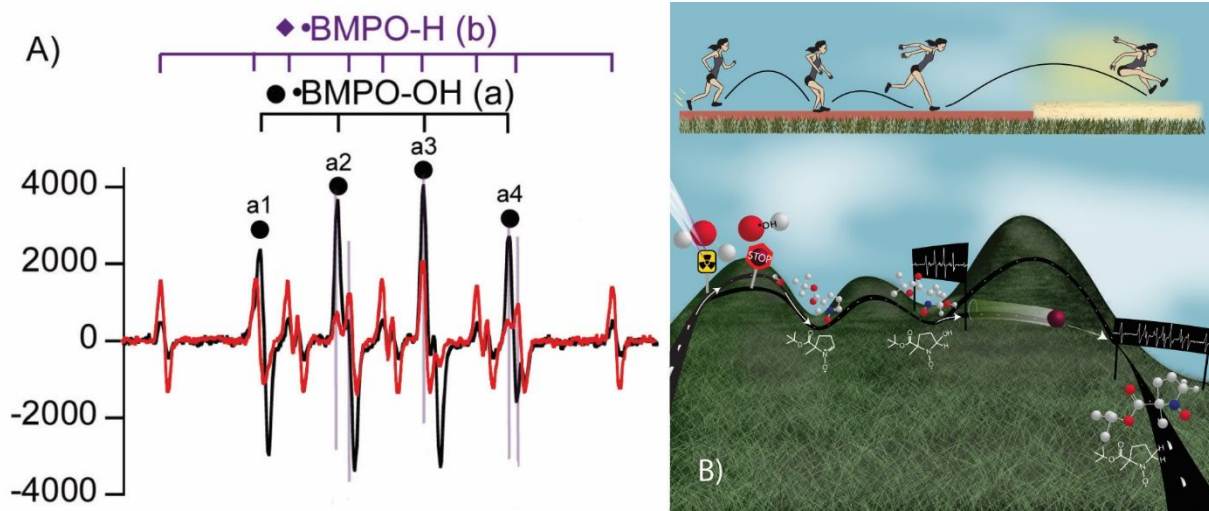


Figure 8. Demonstration of type 1 chemical enhancement (T1CE). A) displays the conversion of $\bullet\text{BMPO-OH}$ (black trace) to $\bullet\text{BMPO-H}$ (red trace). The catalytic conversion is enabled by 3-nm gold nanoparticles (AuNPs). In this measurement, the conversion is caused by mixing X-ray irradiated BMPO (aq.) with the AuNPs, which excludes the participation of OH radicals, therefore proving that the enhancement has nothing to do with ROS production. The enhancement, which can be calculated as the ratio of the height of signals for the left most peaks with to without AuNPs, is approximately 1.4 DEU (abs). B) shows a triple-jump model to elucidate the reaction pathways responsible for the conversion, which occurs in the third phase. The model showcases why the total distance or the yield of product is not necessarily dependent of only the first phase.³⁵

In another example, nanoparticles are shown to cause enhancement to a dosimetric reaction, hydroxylation of 3-CCA to 7-OHCCA.²⁹ Gold nanoparticles are shown to cause increased production of 7-OHCCA after a mixture of 3-CCA and gold nanoparticle aqueous solution is exposed X-ray irradiation. Since the same gold nanoparticles used in the BMPO study mentioned above are used here, no additional production of $\bullet\text{OH}$ is predicted. The enhancement is thus predicted to be caused by the interaction of 3-CCA- $\bullet\text{OH}^*$ radical intermediate with the gold surface, similar to the AuNP catalyzed conversion of $\bullet\text{BMPO-OH}$ to $\bullet\text{BMPO-H}$ discussed above.

Other reports also show increased chemical reaction yields without explicitly invoking the need for increased production of ROS. For example, results appearing in several reports suggest that DNA strand break reactions may be catalyzed.³⁶ In one report, 3-nm gold nanoparticles are used, and the AuNPs are in contact with the DNA strands through direct chemical conjugation.³⁶ It is found that only 20% of the 2.0 DEU enhancement could be explained by T2PE, whereas the other 80% is unaccounted for. T1CE may be responsible for this portion of the enhancement. In a similar experiment, the amount of DNA strand breaks also surpass the predicted yield.⁸ In yet another report demonstrating T1CE, polymerization of aniline is found to be catalyzed by $\bullet\text{OH}$ interacting with Ag/Au core-shell nanostructures.³⁷ The measured enhancement is on the order of 38 DEU when the yield of polymerization on the surface of the nanostructures under X-ray irradiation is compared to spontaneous polymerization on the surface without X-ray irradiation. The enhancement is nearly 400 DEU when the yield is compared to polymerization under X-ray irradiation without the nanostructures. No direct $\bullet\text{OH}$ measurements are performed in any of these works due to lack of experimental tools.

3.2.3. Type 2 Chemical Enhancement

CE may also cause an increased production of ROS, which can be produced by nanomaterials even without X-rays.³⁸ For example, superoxide radicals are found to be produced from molecular oxygen in solutions via interactions with the gold surface.³⁸ Under X-ray irradiation of samples with the added nanomaterials, many reports have claimed to have measured increased production of ROS.^{29-30, 39} One must, however, be cautioned that these claims of observing increased production of ROS are often not

based on direct measurements of ROS but through indirect detection of the products of chemical reactions between probes and ROS, as shown in the last section. The enhancement can be called type 2 chemical enhancement (T2CE) when the nanomaterials catalytically increase the production of ROS. Figure 9 shows two possible pathways of T2CE. One is through nanomaterials directly absorbing X-rays. A similar hypothesis is mentioned in a recent publication, which relies on the absorption of characteristic X-rays emitted from gold nanoparticles by other nanoparticles.³⁰ The second pathway is AuNPs interacting with Compton electrons produced from water scattering X-rays. However, none of these pathways have not been directly verified.

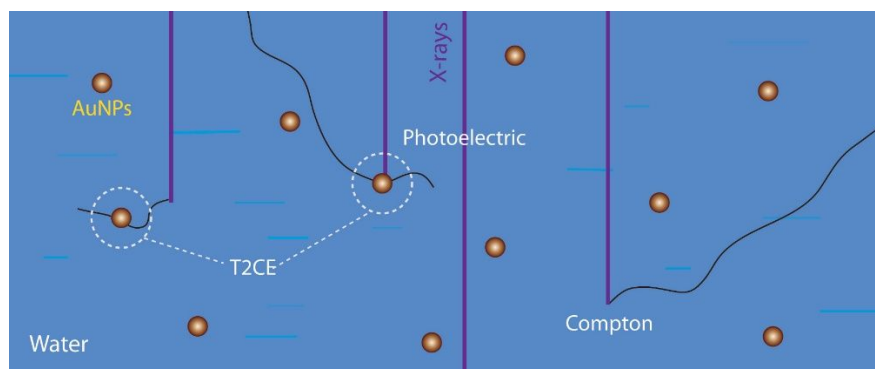


Figure 9. Suggested pathways for type 2 chemical enhancement (T2CE). The production of OH radicals is enhanced at the surface of the gold nanoparticles excited by electrons (likely) or fluorescent X-rays (unlikely). The latter is unlikely because the flux of fluorescent X-rays should be much weaker than the incident X-rays and the absorption of characteristic X-rays emitted from gold by gold should be minimal. Three X-ray absorption events are shown: i) by water and the Compton electron that interact with AuNPs ii) by AuNPs and iii) by water and Compton electrons that do not interact with any AuNPs. The first two events generate T2CE and the third produces background.

In one report, it is found that the yield of hydroxyl and superoxide radical production are increased when gold nanoparticles of different sizes, ranging from 10 nm to 250 nm, are used.³⁰ The increase, which is measured using dosimetric reactions and therefore are an indirect approach, is found to be dependent of the radius of the gold nanoparticles. Therefore, catalytic properties of the nanomaterials are invoked. The enhancement is categorized into T2CE because an increased ROS production is claimed. In two other reports, which are also discussed in the T1CE section, similar dosimetric reactions are used and similar results are obtained. Again, the cause for the enhancement is attributed to the increased production of ROS.³⁹ In a fourth report, a water layer on the surface of the gold nanoparticles is claimed to be the cause for the enhancement.⁴⁰ All these T2CE cases shown in the literature to date could be categorized into T1CE as well if eventually ROS production is found to remain constant and the actual change is the catalytic conversion of intermediates to the final products.

3.2.3.1. Anti-Enhancement

At high enough gold nanoparticle concentrations, anti-enhancement (AE) could appear or even dominate. In these cases, AE is assigned to T2CE because the amount of ROS is changed. At low AuNP concentrations, ROS - AuNPs interactions are weak and most of the ROS react with probes, thus keeping AE insignificant. Only when the gold nanoparticle concentrations are high enough, do ROS begin to directly react with nanoparticles. This phenomenon has been observed by many groups.³¹⁻³⁴ In the EPR report mentioned above, for example, OH radicals are weakly scavenged by small AuNPs.³⁵

3.2.4. Difference between Physical and Chemical Enhancements

T2PE and CE can be differentiated experimentally by coating a thin inert layer of materials on large gold nanoparticles to eliminate CE while maintaining T2PE. On the other hand, very small (< 5 nm), catalytically active nanoparticles possess CE but little T2PE. Future work is needed to exclusively

demonstrate CE without T2PE, and vice versa. Other parameters such as dose rates can also be used to vary CE but not T2PE. X-ray energy can also be used to change T2PE.^{15, 24} It is understandable that X-ray energy should also influence CE, although such dependency has not been quantitatively studied yet.

3.2.5. *Applications of Chemical Enhancement*

CE is available when the surface of nanomaterials is exposed to the reactions of interest. This means that CE should exist in many cases. However, it is critical to examine the surface coverage when CE is planned even though pristine nanoparticles with known catalytic properties could support CE. The surface is often blocked after the nanomaterials are exposed to the environment, leading to unintended results. Recent work has shown that CE may be combined with large surface area materials such as metal-organic framework (MOF) materials to generate ROS.⁴¹ Future work is needed to preserve and expand CE capabilities of nanoparticles in practical environments.

3.3. Biological Enhancement

3.3.1. *Introduction*

Biology consists of an enormously large set of chemical reactions happening simultaneously within tight spaces. There are often simultaneously multiple sets of reactions at the same physical location. Knowing how difficult it can be to fully understand a relatively simple chemical reaction such as the hydroxylation reaction of 3-CCA in the presence of nanoparticles as described in Section 3.2.2, it is difficult to fathom that we can actually understand what happens in cells under X-ray irradiation in the presence of nanoparticles, which can be much more complex than X-ray irradiation of cells alone. Nanoparticles can also scavenge, so there is no guarantee that adding nanoparticles would cause any enhanced production of ROS in cells. Beyond all these enhancements and anti-enhancements, cells also have intrinsic defense mechanisms to defend against ROS produced by X-ray irradiation of nanoparticles, and X-ray produced ROS may activate these defense mechanisms and cause biological anti-enhancement or hormesis in the presence of nanomaterials.⁴²

A strong evidence for cellular amplification/regulation of the actions by nanomaterials and X-rays is shown in Figure 10, which presents the results of many studies of responses (solid circles) and the predicted T1PE (dashed line) based on the absorption of X-rays by nanomaterials in the cell through uptake.¹ Similar presentations have been shown in the literature, although here the range of nanomaterial concentration is broader.³ The measured cellular responses seem to be approximately 1.0 DEU, regardless of the amount of nanomaterials in the system that is over the span of five orders of magnitude. These results clearly demonstrate the complexity of biological responses to the addition of even relatively simple nanomaterials and X-ray irradiation, and that biological responses depend on many factors beyond weight percentage and size of nanomaterials. It is important to point out that it is possible that after PE and CE, including AE, are all included, the difference between the predicted total enhancement may not be as drastically different from the measured enhancements (Figure 10).

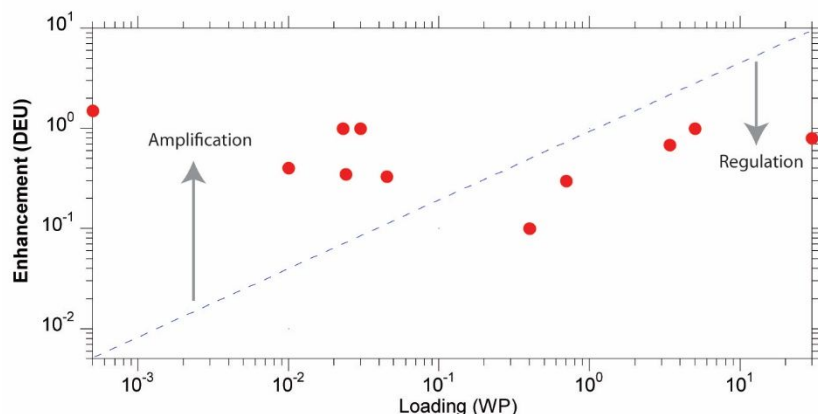


Figure 10. Evidence for biological enhancement (BE). The experimental data (solid dots) and predicted T1PE (dotted line) are shown. Clearly there is little correlation between the two. In addition, the measured enhancement values (without standard deviations) are largely between 0.1 and 1.0 DEU, suggesting strong cellular regulation over the enhancement. Graph adapted from ref ¹.

Given the complexity of the biological systems, it is reasonable to conclude that there are many biological reaction pathways that are altered by the added nanomaterials, therefore causing enhancements going beyond physical and chemical enhancements described in previous sections. It is therefore reasonable to invoke a new category of enhancement called biological enhancement (BE) that can specifically address the response from biological systems upon uptake of nanoparticles and irradiation of X-rays.

Similar to physical and chemical enhancements, there could also be several types of BE. It is possible to define type 1 biological enhancement as the enhancement caused by nanomaterials that cannot possibly cause any known chemical or physical enhancement. It can also be interpreted that type 1 biological generate does not cause any direct damage to biological targets by the added nanomaterials under X-ray irradiation. In contrast, type 2 biological enhancement is the biologically amplified damage caused by either chemical or physical enhancement or both. Without the biological systems, there will be no change to damage to the targets generated by the chemical or physical enhancement or both. In both cases, it is critical to realize that BE goes beyond and is different from PE and CE.

3.3.2. Type 1 Biological Enhancement

As described above, type 1 biological enhancement (T1BE) does not require nanomaterials to directly damage biological targets under X-ray irradiation, even though there is more damage to the whole system (cells or animals) by X-ray irradiation in the presence of nanomaterials. For example, nanomaterials impeding the function of DNA repair proteins do not cause direct damage to the proteins, but such non-damaging hindrance can cause more damage to the cell because these cells cannot properly repair double strand breaks of nuclear DNA caused by X-rays. The enhancement is acquired through reaction pathways affected by nanomaterials, which cause damage to secondary targets, no enhanced damage occurs to the primary targets by nanomaterials under X-ray irradiation. T1BE is most likely caused by inert nanomaterials targeting certain biological pathways and not biological targets themselves. An illustration of T1BE is given in Figure 1, which shows a nanoparticle hindering the function of a DNA repair protein (SUMO). The reason for naming this type of enhancement T1BE is because to date this enhancement is more frequently reported in the literature.

In one example, 2 nm gold nanoparticles are used to target a DNA damage repair protein SUMO (Figure 11A).⁴³ The damage to the protein through PE at the reported dose of 6 Gy would be minimal to the proteins and should be below the detection limit based on damage to other proteins such as GFP. CE to

the damage of the protein is possible, but the dose employed is still too low to cause any measurable damage to the proteins. The most sensible explanation is gold nanoparticles targeting the repair proteins to hinder the repair of the damaged DNA by X-rays alone. Barring direct damage to DNA by nanomaterials, the report evinces T1BE.

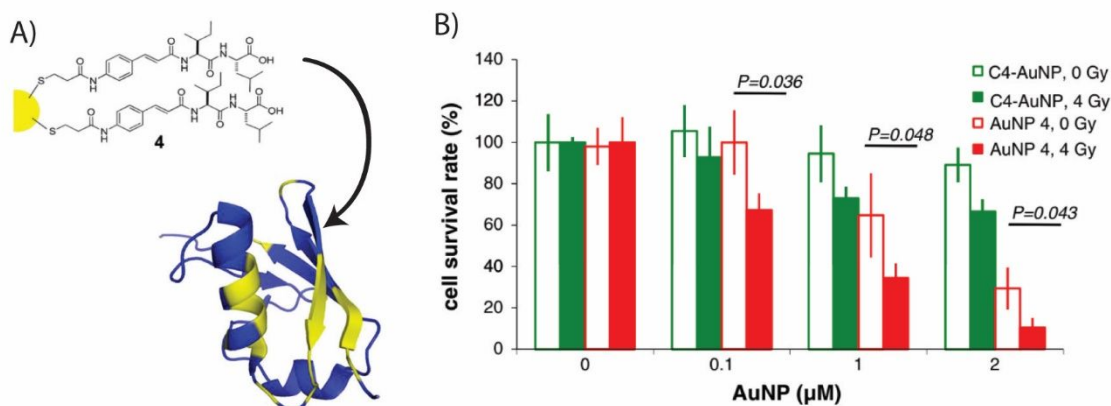


Figure 11. Illustration of type 1 biological enhancement (T1BE). A) presents a DNA repair protein SUMO, which is targeted by the NSC311751 ligand covering gold nanoparticles (AuNPs). 2 nm AuNPs are used in this work. B) displays the results of damage by the gold nanoparticles (AuNP 4) under X-ray irradiation. Adapted from ref ⁴³.

Evidence of T1BE is also given in the study using 29-43 atom gold nanoparticles to generate 1.0 DEU enhancement in cell damage measured in survival fractions.⁴⁴ Due to their small sizes and low concentrations (100 ppm), X-ray absorption by these nanoparticles is minimal, therefore generating negligible PE. It is unlikely that such small nanoparticles can generate CE due to the coverage of large ligands on the surface of these AuNPs. The observed enhancement thus should be caused by BE without direct damage to any targets.

In another but less conclusive example, enhancement is demonstrated using 1.9 nm AuNPs without targeting ligands on the surface to interact with protein disulfide isomerase (PDI) to disrupt thiol balance in cells, therefore causing a ROS imbalance and oxidative stress to mitochondria.⁴⁵ The final target to damage is mitochondria, although such damage is not directly caused by AuNPs and X-ray irradiation. In this sense, there should be no CE or PE, although these enhancements are not explicitly excluded.

3.3. Type 2 Biological Enhancement

In T1BE, there is no direct damage to biological targets by nanomaterials under X-ray irradiation even though there is an increased damage to the whole system through the introduction of nanomaterials. This is to a degree similar to T1CE in which no additional ROS is produced by the nanomaterials under X-ray irradiation and yet the overall chemical reactivity is enhanced. In T1BE, the damage to the biological system is increased because the nanomaterials affect the biological pathways responsive to X-ray irradiation.

In type 2 biological enhancement (T2BE), there is an increased damage to biological targets caused by nanomaterials under X-ray irradiation through CE or PE or both, and this damage is further enhanced or amplified biologically. More precisely, if the magnitude of overall biological damage is the same as or below the damage to the component(s), then the damage should be categorized as PE or CE and not T2BE because there is no further biological involvement. If, on the other hand, there is damage to the targets, *and* the enhancement to the whole system is greater than the damage to the targets, then there is T2BE. The targets of T2BE can be DNA, RNA, proteins, mitochondria, enzymes, endoplasmic

reticulum (ER) or other biological components. There could also be biological anti-enhancement, that is, if the magnitude of damage to the whole system is significantly less than to a component.

There are a limited number of reports in the literature that carry out measurements of damage to both the targets and the cells. The results are listed in Table 3. Among them only two reports have detected greater damages to the system than to the target.⁴⁶⁻⁴⁷ In the first report, nuclear DNA damage is detected using γ -H2AX assay and the system damage in terms of surviving fraction is detected using the clonogenic assay, and the two enhancements are 0.43 and 1.43 DEU, respectively, suggesting that the direct damage of nuclear DNA is amplified by the cell. It is possible, however, that this result also contains T1BE because the nanoparticles may also hinder the repair function. Another example that shows T2BE is via targeted damage to Caspase-3 activation by bursts of ROS associated with irradiation of TiO₂-Au nanoparticles with X-rays.⁴⁷ The nanomaterials are 3-5 nm AuNPs decorated on 18 nm TiO₂ nanoparticles. Superoxide radicals were probed by an ROS assay using DBZTC, a dosimetric reaction that can also be catalyzed by the AuNPs. The increase of superoxide radicals and mitochondrial oxygen consumption rate (OCR) are 2.0 and 4.0 DEU. The damage is also assessed by membrane polarization changes that lead to dysfunction in mitochondria damage. The damage to the whole system, determined by clonogenic assay, is 6.5 DEU, giving rise to approximately 0.62 DEU T2BE. The surviving fraction (SF) obtained in this work is 85% after 4 Gy of X-ray irradiation, higher than the average SF of 37%. These results are also listed in Table 3. A closely related third example is reported recently in which nuclear DNA damage is detected by the γ -H2AX assay and the system damage in terms of surviving fraction detected by the clonogenic assay.⁴⁸ In that example, however, the two enhancements are almost identical. The results are also listed in Table 3.

There are many reports that have presented both target and system damage values, but the system damages are lower than the magnitude of target damage. Table 3 lists four such examples that show negative T2BE. In the first example, 50 nm gold nanoparticles (AuNPs) are employed and nuclear DNA damage measured with γ -H2AX assay shows an enhancement of 0.79 DEU and cell surviving fraction determined by the clonogenic assay has a 0.43 DEU enhancement, resulting in a -0.46 DEU T2BE.⁴⁹ Another report uses peptide targeting ligands (CCYKFR) to assist damage to mitochondria by 3-nm AuNPs.⁵⁰ The results show a 14-fold increase in ROS production in cells by CCYKFR-conjugated AuNPs using a fluorescent assay and a 4.0-fold increase in nuclear DNA damage using γ -H2AX assay. The cell survival fraction is only 0.90 DEU, which is lower than the magnitude of DNA damage. In the third work, approximately 100 nm micelles filled with 1.9 nm AuNPs are used to generate DNA and cell damage.⁵¹ However, the damage to the system again is smaller than to the target. The fourth example of negative T2BE presented in Table 3 shows that ROS production measured in the cell is increased by 62%, or in a 0.62-DEU enhancement, whereas SF is only reduced by 8%, giving rise to a 0.87-DEU T2BE.⁵²

Table 3. Evidence for the existence of T2BE. Only those studies that have measured both the targets and the whole biological systems are discussed. Among these studies, only two reports show evidence for T2BE (black); the rest have negative T2PE (light grey). Enhancements are absolute enhancements.

Target Damage by NMs under X-rays (γ -H2AX)	System Damage (clonogenic)	Nanomaterials and dimensions (nm)	Be ^a	Ref
0.43	1.43	4 nm Gd ₂ O ₃ /SiO ₂	2.3	46
4.0	6.5	18 nm AuNP@TiO ₂ NPs	0.62	47
1.46	1.47	50-70 nm TiO ₂ NPs	0.0	48
0.79	0.43	50 nm AuNPs	-0.46	49

4.0	0.90	3 nm AuNPs	-0.78	50
1.50	0.40	Micelles of 1.9 nm AuNPs	-0.73	51
0.62	0.08	14 nm AuNPs	-0.87	52

a) absolute enhancement, in units of DEU.

3.3.4. Other Types of Biological Enhancement

Other factors or processes can influence how biological systems respond to irradiation of X-rays in the presence of nanomaterials. One of these factors is cell type, which may affect how the cell regulates the damage to the targets and signaling pathways. Many cell lines have been tested, and despite using the same nanoparticles and irradiation protocols, the measured enhancements vary significantly for different cell lines.^{1, 53-55} Specifically, certain cells (e.g., MCF-7 breast cancer cell line) lacking caspase-3 activation to signal and regulate the damaged cellular components permit these cells to survive with mutations whereas damaged cells of other cell types may undergo apoptosis (p53 dependent apoptosis).⁵⁶⁻⁵⁷ The second factor is cell cycle. For example, delayed G2/M stage is shown to improve uptake of nanomaterials.⁵⁸ Therefore, an initial dose of irradiation to cause this delay followed by incubation of AuNPs and another dose of irradiation can possibly increase the uptake and damage to the cell. Endoplasmic reticulum (ER) and protein folding have also been cited as biological targets.⁴ There is also a bystander effect, which causes the irradiated cells to release signaling chemicals to affect the unirradiated cells.⁵⁹⁻⁶⁰ A similar process called abscopal effect is also being examined.⁶¹

3.3.5. Applications of Biological Enhancement

BE has just begun to be explored and utilized. It is possible that most nanomaterials can cause some kind of BE, even though researchers may not know it. Furthermore, it is difficult to initiate BE because of the complexity of the biological systems. Future work is needed to develop more advanced nanomaterials and targeting routes to exclusively engage BE.

3.4. Combinations of Enhancements

Different enhancements can coexist. For example, physical and chemical enhancements both occur when some common nanomaterials are used together. Here, three ways of combining enhancements are discussed.

3.4.1. Isolation of Enhancement

As shown in previous sections, carefully prepared nanomaterials may invoke specific category, type or kind of enhancement. Isolation of these enhancements is difficult, although not impossible. There are several cases where such isolation is possible, and these reports are given in the previous sections.

3.4.2. Addition

As defined here and elsewhere, T1PE is uniform everywhere and T2PE is the strongest at the surface of nanomaterials. Both are caused by the electrons emitted from the nanomaterials as a result of X-ray absorption by the nanomaterials. If the two can be measured independently, then the total enhancement should follow a simple addition algorithm with respect to the two individual enhancements. An example is given in a recent report in which the probes, which are calcium phosphate enclosed liposomes (CaPELs) filled with an aqueous solution of dye molecules, become attached to gold nanoparticles when the concentration of the AuNPs in water is greater than 0.25 WP.¹⁷ As the concentration increases beyond this threshold, heterodimers form between the AuNPs and CaPEL probes, generating T2PE in the probe. T1PE, on the other hand, exists at all concentrations and has a slope of 1.0 DEU WP⁻¹. Therefore, above 0.25 WP, the total enhancement is the addition of T1PE and

T2PE. For example, at 0.3 WP, the total enhancement is 2.25 DEU, among which 2.0 DEU is contributed from T2PE and 0.25 DEU is from T1PE for 0.25 WP AuNPs.

3.4.3. Subtraction

AE generally reduces enhancement because the nanoparticles scavenge ROS. This reduction of ROS translates to subtraction of reaction yields by AE.

3.4.4. Multiplication

When CE and PE coexist, the algorithm for the total enhancement with respect to the two individual enhancements can be multiplication, which is demonstrated in a recent report.⁶² In this example, T1CE and T1PE are created by 3-nm small gold nanoparticles and large silica-coated 100 nm gold nanoparticles, respectively. 3-nm gold nanoparticles are known to cause strong T1CE.²⁹ The 8-nm thick silica-coated 100-nm gold nanoparticles generate strong T1PE without exposing catalytic surface of gold nanoparticles.⁹ When mixed, the small gold nanoparticles are uniformly distributed in the solution and are not on the surface of silica-coated large AuNPs. As a result, the combined enhancement is largely from T1PE, not T2PE, and T1CE, and the measurements (Figure 12B) confirm the multiplication algorithm between the two enhancements and the total enhancement. It is important to point out that in this multiplication algorithm T1CE is modified by T1PE because CE is dose rate dependent.²⁹ For example, for T1CE of 2.0 DEU (rel) without T1PE, the new T1CE with a 5.0 DEU (rel) T1PE can be as high as 10 DEU if there is no saturation to CE at the T1PE modified dose rate. If the modified T1CE is 10 DEU, then the total enhancement should be 30 DEU, calculated using the equation 5.18 shown in ref 1. This magnitude of enhancement is higher than the measured total enhancement of 18 DEU, indicating some saturation to T1CE at this X-ray dose rate and T1PE. The measured total enhancement is higher than either T1CE or T1PE or the sum/addition of the two (without T1PE correction). Two lines are drawn in Figure 12B to represent the combined enhancements without dose rate dependency (blue) for T1CE and without saturation of dose rate dependency (red). The former is much lower than the latter. The measured enhancements are between these two sets of values.

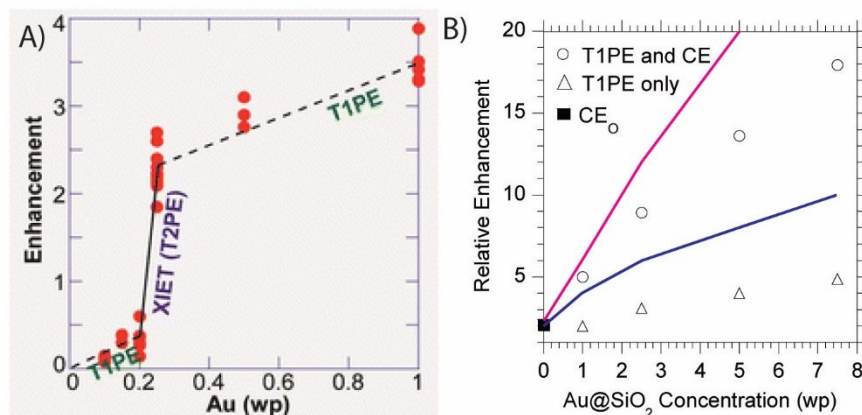


Figure 12. Algorithms for combined enhancements. A) The standard addition algorithm for T1PE and T2PE.¹⁷ B) The standard multiplication algorithm for T1CE and T1PE. T1CE (CE0) shown here is CE without T1PE modification, which is approximately 2.0 DEU (rel) at 0.05 WP for 3-nm AuNPs. T1PE is achieved at several concentrations of silica-coated large AuNPs. Two lines are drawn, the red is the total enhancement calculated using the multiplication algorithm and T1CE that is dose rate dependent and without saturation, and the purple is the obtained using the same algorithm and T1CE that is not dose rate dependent.⁶²

3.4.5. Applications of Combined Enhancement

Most likely all of the reported results contain more than one category of enhancement. If possible, one would want to use the combination of all categories of enhancement to achieve the highest magnitude

of total enhancement. Such combinations can help solve many scientific, technological and societal problems. However, such combinations have not been explored due to many obstacles.

4. Other Advancements in X-ray Nanochemistry

Several application areas are briefly mentioned here, which are based on the three fundamental enhancement processes described in this perspective.

4.1. Materials

Generation of stronger enhancements in X-ray nanochemistry demands new nanomaterials and innovative nanochemistry. For example, nanoreactors could be used to protect dosimetric or other reactions from outside chemical environments that scavenge or catalyze radicals produced by ionizing radiation. One recent development is the synthesis and use of sealable mesoporous silica nanoreactors to probe X-ray doses and enhancements.⁶³

4.2. Instruments

Numerous instruments have been used in studying X-ray nanochemistry. X-ray instruments are largely based on traditional X-ray sources, although it is understandable that more compact, inexpensive X-ray sources will be developed and used because lower doses of X-rays are needed after all these enhancements are optimized. Synchrotrons are used when intense, monochromatic X-rays are needed, which are useful in mechanistic studies. Analytical apparatuses such as MALDI, ICP-MS, EPR, NMR, XPS, and fluorimetry have been used to measure enhancements. Scintillation detection and other optical measurements are efficient methods for enhancement determination. In addition, new instruments are built.⁶⁴ It is certain that more advanced tools and methodologies are needed to detect ROS and reaction products such as DNA strands, proteins, and fluorescent molecules, especially reactive radical intermediates (RRI) related to these products.

4.3. Applications in Biology, Cancer Treatment, Catalysis, and Environment

X-ray nanochemistry is largely originated from studying cancer treatment and over 50% of the publications in the field of X-ray nanochemistry investigate cancer treatment.¹ The effectiveness of the treatment to date ranges from little or no effects to up to an 82-DEU enhancement in terms of tumor suppression/regression attributed to the injected nanoparticles under 10-1000 keV X-ray irradiation.^{1, 65} Given that nanoparticles can be used to target cellular components, it is reasonable to think that X-ray nanochemistry can be used to study biological pathways. An example of such studies is reported recently.⁶⁶ Catalysis can also be studied using X-ray nanochemistry and *vice versa*, and a recent study shows that it is possible to isolate reaction steps and determine the catalytic steps.³⁵ Environmental Science can be a unique application area, as ionizing radiation can be used to break the most environmentally resistive chemicals.⁶⁷

5. Future work

The scope of X-ray nanochemistry is expanding, as indicated by recent publications.¹ New materials have been one of the foci of X-ray nanochemistry research. For example, nanoreactors have been reported in recent years.⁶³ When fully developed, these reactors may serve many purposes including characterization of X-ray induced energy transfer (XIET).²⁴ New instrumentation and methodologies are being developed as well, which may see significant improvements in the next decade of X-ray nanochemistry research, as the current methods and tools are still limited and many properties and mechanisms are still being speculated. For example, many ROS assays can be affected by nanomaterials, and yet such impact has only been studied in limited manners due to a lack of direct measurements of OH radicals. Future work will help conclusively determine the reaction pathways and provide the knowledge basis for improvement. Ultrafast spectroscopy and possibly *in situ* transmission electron

microscopy (TEM) are the tools that may assist the study of dynamics and mechanisms. In addition, new quantum chemistry theories will be needed to help fully comprehend, guide and predict how nanomaterials interact with ROS and reactive radical intermediates created under X-ray irradiation in complex chemical and nanochemical systems.

6. Conclusions

X-ray nanochemistry is a new discipline of research. It began two decades ago with simply mixing nanomaterials with other chemicals or placing nanomaterials in cells or animals to increase the X-ray dose factor. However, adding nanomaterials does not always induce enhancement unless certain conditions are met. X-ray nanochemistry investigates how to create the best conditions for the highest enhancement based on the fundamental physical chemistry properties. The categorization of enhancement to the X-ray effects described in this perspective is one way to simplify these complex processes in X-ray nanochemistry. Physical, chemical and biological enhancements are created based on their intrinsic natures governing the interactions between nanomaterials and systems under X-ray irradiation that bring about the enhancement. These categorizations may change and expand over time, as more categories, types and kinds of enhancement are discovered and developed. The highest enhancements will most likely be accomplished when high individual enhancements are properly combined.

Acknowledgements

The author thanks the support by the National Science Foundation (CHE-1307529) and the assistance of Ms. Mengqi Su, Dr. Arjun Sharmah and Dr. Jennifer Lien.

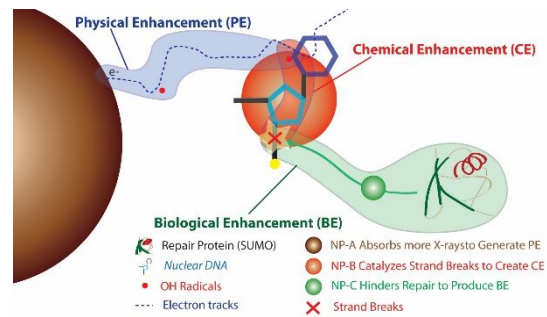
References

1. Guo, T., *X-ray nanochemistry : concepts and development*. Springer International Publishing: New York, NY, 2018; p XXI, 513.
2. Ciccia, A.; Elledge, S. J., The DNA Damage Response: Making It Safe to Play with Knives. *Mol Cell* **2010**, *40* (2), 179-204.
3. Butterworth, K. T.; McMahon, S. J.; Currell, F. J.; Prise, K. M., Physical basis and biological mechanisms of gold nanoparticle radiosensitization. *Nanoscale* **2012**, *4* (16), 4830-4838.
4. Brun, E.; Sicard-Roselli, C., Actual questions raised by nanoparticle radiosensitization. *Radiation Physics and Chemistry* **2016**, *128*, 134-142.
5. Her, S.; Jaffray, D. A.; Allen, C., Gold nanoparticles for applications in cancer radiotherapy: Mechanisms and recent advancements. *Advanced Drug Delivery Reviews* **2017**, *109*, 84-101.
6. Cho, S. H., Estimation of tumour dose enhancement due to gold nanoparticles during typical radiation treatments: a preliminary Monte Carlo study. *Physics in Medicine and Biology* **2005**, *50* (15), N163-N173.
7. Leung, M. K. K.; Chow, J. C. L.; Chithrani, B. D.; Lee, M. J. G.; Oms, B.; Jaffray, D. A., Irradiation of gold nanoparticles by x-rays: Monte Carlo simulation of dose enhancements and the spatial properties of the secondary electrons production. *Med Phys* **2011**, *38* (2), 624-631.
8. McMahon, S. J.; Hyland, W. B.; Brun, E.; Butterworth, K. T.; Coulter, J. A.; Douki, T.; Hirst, D. G.; Jain, S.; Kavanagh, A. P.; Krpetic, Z.; Mendenhall, M. H.; Muir, M. F.; Prise, K. M.; Requardt, H.; Sanche, L.; Schettino, G.; Currell, F. J.; Sicard-Roselli, C., Energy Dependence of Gold Nanoparticle Radiosensitization in Plasmid DNA. *J Phys Chem C* **2011**, *115* (41), 20160-20167.
9. Davidson, R. A.; Guo, T., Average Physical Enhancement by Nanomaterials under X-ray Irradiation. *J Phys Chem C* **2014**, *118* (51), 30221-30228.
10. Chang, J.; Taylor, R. D.; Davidson, R. A.; Sharmah, A.; Guo, T., Electron Paramagnetic Resonance Spectroscopy Investigation of Radical Production by Gold Nanoparticles in Aqueous Solutions Under X-ray Irradiation. *J Phys Chem A* **2016**, *120* (18), 2815-2823.
11. Abolfazi, M. K.; Mahdavi, S. R.; Mahdavi, M.; Gh, A., Studying Effects of Gold Nanoparticle on Dose Enhancement in Megavoltage Radiation. *J. Biomed. Phys. Eng.* **2015**, *5* (4), 185-190.
12. Paudel, N.; Shvydka, D.; Parsai, E. I., Comparative Study of Experimental Enhancement in Free Radical Generation against Monte Carlo Modeled Enhancement in Radiation Dose position Due to the Presence of High Z Materials during Irradiation of Aqueous Media. *International Journal of Medical Physics, Clinical Engineering and Radiation Oncology* **2015**, *4*, 300-307.
13. McMahon, S. J.; Paganetti, H.; Prise, K. M., Optimising element choice for nanoparticle radiosensitisers. *Nanoscale* **2016**, *8* (1), 581-589.
14. Carter, J. D.; Cheng, N. N.; Qu, Y. Q.; Suarez, G. D.; Guo, T., Nanoscale energy deposition by x-ray absorbing nanostructures. *J. Phys. Chem. B* **2007**, *111* (40), 11622-11625.
15. Lee, C.; Cheng, N. N.; Davidson, R. A.; Guo, T., Geometry Enhancement of Nanoscale Energy Deposition by X-rays. *J. Phys. Chem. C* **2012**, *116* (20), 11292-11297.
16. McMahon, S. J.; Hyland, W. B.; Muir, M. F.; Coulter, J. A.; Jain, S.; Butterworth, K. T.; Schettino, G.; Dickson, G. R.; Hounsell, A. R.; O'Sullivan, J. M.; Prise, K. M.; Hirst, D. G.; Currell, F. J., Nanodosimetric effects of gold nanoparticles in megavoltage radiation therapy. *Radiother Oncol* **2011**, *100* (3), 412-416.
17. Sharmah, A.; Yao, Z.; Lu, L.; Guo, T., X-ray-Induced Energy Transfer between Nanomaterials under X-ray Irradiation. *J Phys Chem C* **2016**, *120* (5), 3054-3060.
18. Jones, B. L.; Krishnan, S.; Cho, S. H., Estimation of microscopic dose enhancement factor around gold nanoparticles by Monte Carlo calculations. *Med Phys* **2010**, *37* (7), 3809-3816.

19. Ngwa, W.; Makrigiorgos, G. M.; Berbeco, R. I., Gold nanoparticle enhancement of stereotactic radiosurgery for neovascular age-related macular degeneration. *Physics in Medicine and Biology* **2012**, *57* (20), 6371-6380.
20. Hossain, M.; Su, M., Nanoparticle Location and Material-Dependent Dose Enhancement in X-ray Radiation Therapy. *J Phys Chem C* **2012**, *116* (43), 23047-23052.
21. Zygmanski, P.; Liu, B.; Tsiamas, P.; Cifter, F.; Petersheim, M.; Hesser, J.; Sajo, E., Dependence of Monte Carlo microdosimetric computations on the simulation geometry of gold nanoparticles. *Physics in Medicine and Biology* **2013**, *58* (22), 7961-7977.
22. Zabihzadeh, M.; Moshirian, T.; Ghorbani, M.; Knaup, C.; Behrooz, M. A., A Monte Carlo study on dose enhancement by homogenous and inhomogeneous distributions of gold nanoparticles in radiotherapy with low energy X-rays. *J. Biomed. Phys. Eng.* **2016**, I-XVI.
23. Su, M. Q.; Guggenheim, K. G.; Lien, J.; Siegel, J. B.; Guo, T., X-ray-Mediated Release of Molecules and Engineered Proteins from Nanostructure Surfaces. *Acs Appl Mater Inter* **2018**, *10* (38), 31860-31864.
24. Sharmah, A.; Lien, J.; Su, M. Q.; Guo, T., Theoretical Study of X-ray Induced Energy Transfer (XIET) from Nanomaterial Donors to Nanomaterial Acceptors. *J Phys Chem C* **2018**, *122* (32), 18640-18650.
25. Meer, B. W. v. d., *FRET - Forster Resonance Energy Transfer: From Theory to Applications*. Wiley-VCH/Verlag GmbH & Co. KGaA: Weinheim, Germany, 2014.
26. Kamkaew, A.; Chen, F.; Zhan, Y. H.; Majewski, R. L.; Cai, W. B., Scintillating Nanoparticles as Energy Mediators for Enhanced Photodynamic Therapy. *Acs Nano* **2016**, *10* (4), 3918-3935.
27. Davidson, R. A.; Sugiyama, C.; Guo, T., Determination of Absolute Quantum Efficiency of X-ray Nano Phosphors by Thin Film Photovoltaic Cells. *Anal Chem* **2014**, *86* (20), 10492-10496.
28. Gara, P. M. D.; Garabano, N. I.; Portoles, M. J. L.; Moreno, M. S.; Dodat, D.; Casas, O. R.; Gonzalez, M. C.; Kotler, M. L., ROS enhancement by silicon nanoparticles in X-ray irradiated aqueous suspensions and in glioma C6 cells. *Journal of Nanoparticle Research* **2012**, *14* (3).
29. Cheng, N. N.; Starkewolf, Z.; Davidson, R. A.; Sharmah, A.; Lee, C.; Lien, J.; Guo, T., Chemical Enhancement by Nanomaterials under X-ray Irradiation. *J Am Chem Soc* **2012**, *134* (4), 1950-1953.
30. Misawa, M.; Takahashi, J., Generation of reactive oxygen species induced by gold nanoparticles under x-ray and UV Irradiations. *Nanomedicine-Nanotechnology Biology and Medicine* **2011**, *7* (5), 604-614.
31. Hamasaki, T.; Kashiwagi, T.; Imada, T.; Nakamichi, N.; Aramaki, S.; Toh, K.; Morisawa, S.; Shimakoshi, H.; Hisaeda, Y.; Shirahata, S., Kinetic analysis of superoxide anion radical-scavenging and hydroxyl radical-scavenging activities of platinum nanoparticles. *Langmuir* **2008**, *24* (14), 7354-7364.
32. He, W. W.; Zhou, Y. T.; Warner, W. G.; Hu, X. N.; Wu, X. C.; Zheng, Z.; Boudreau, M. D.; Yin, J. J., Intrinsic catalytic activity of Au nanoparticles with respect to hydrogen peroxide decomposition and superoxide scavenging. *Biomaterials* **2013**, *34* (3), 765-773.
33. Nie, Z.; Liu, K. J.; Zhong, C. J.; Wang, L. F.; Yang, Y.; Tian, Q.; Liu, Y., Enhanced radical scavenging activity by antioxidant-functionalized gold nanoparticles: A novel inspiration for development of new artificial antioxidants. *Free Radical Bio Med* **2007**, *43* (9), 1243-1254.
34. Watanabe, A.; Kajita, M.; Kim, J.; Kanayama, A.; Takahashi, K.; Mashino, T.; Miyamoto, Y., In vitro free radical scavenging activity of platinum nanoparticles. *Nanotechnology* **2009**, *20* (45).
35. Lien, J.; Su, M. Q.; Guo, T., Identification of Individual Reaction Steps in Complex Radical Reactions Involving Gold Nanoparticles. *Chemphyschem* **2018**, *19* (24), 3328-3333.
36. Carter, J. D.; Cheng, N. N.; Qu, Y. Q.; Suarez, G. D.; Guo, T., Enhanced single strand breaks of supercoiled DNA in a matrix of gold nanotubes under X-ray irradiation. *J. Colloid Interf. Sci.* **2012**, *378*, 70-76.

37. Davidson, R. A.; Guo, T., An Example of X-ray Nanochemistry: SERS Investigation of Polymerization Enhanced by Nanostructures under X-ray Irradiation. *J Phys Chem Lett* **2012**, *3* (22), 3271-3275.
38. Ionita, P.; Gilbert, B. C.; Chechik, V., Radical mechanism of a place-exchange reaction of an nanoparticles. *Angew Chem Int Edit* **2005**, *44* (24), 3720-3722.
39. Sicard-Roselli, C.; Brun, E.; Gilles, M.; Baldacchino, G.; Kelsey, C.; McQuaid, H.; Polin, C.; Wardlow, N.; Currell, F., A New Mechanism for Hydroxyl Radical Production in Irradiated Nanoparticle Solutions. *Small* **2014**, *10* (16), 3338-3346.
40. Gilles, M.; Brun, E.; Sicard-Roselli, C., Quantification of hydroxyl radicals and solvated electrons produced by irradiated gold nanoparticles suggests a crucial role of interfacial water. *J Colloid Interf Sci* **2018**, *525*, 31-38.
41. He, Z.; Huang, X. L.; Wang, C.; Li, X. L.; Liu, Y. J.; Zhou, Z. J.; Wang, S.; Zhang, F. W.; Wang, Z. T.; Jacobson, O.; Zhu, J. J.; Yu, G. C.; Dai, Y. L.; Chen, X. Y., A Catalase-Like Metal-Organic Framework Nanohybrid for O₂-Evolving Synergistic Chemoradiotherapy. *Angew Chem Int Edit* **2019**, *58*, 8752-8756.
42. Shibamoto, Y.; Nakamura, H., Overview of Biological, Epidemiological, and Clinical Evidence of Radiation Hormesis. *Int J Mol Sci* **2018**, *19* (8).
43. Li, Y. J.; Perkins, A. L.; Su, Y.; Ma, Y. L.; Colson, L.; Horne, D. A.; Chen, Y., Gold nanoparticles as a platform for creating a multivalent poly-SUMO chain inhibitor that also augments ionizing radiation. *Proceedings of the National Academy of Sciences of the United States of America* **2012**, *109* (11), 4092-4097.
44. Zhang, X. D.; Luo, Z. T.; Chen, J.; Song, S. S.; Yuan, X.; Shen, X.; Wang, H.; Sun, Y. M.; Gao, K.; Zhang, L. F.; Fan, S. J.; Leong, D. T.; Guo, M. L.; Xie, J. P., Ultrasmall Glutathione-Protected Gold Nanoclusters as Next Generation Radiotherapy Sensitizers with High Tumor Uptake and High Renal Clearance. *Sci Rep-Uk* **2015**, *5*.
45. Taggart, L. E.; McMahon, S. J.; Butterworth, K. T.; Currell, F. J.; Schettino, G.; Prise, K. M., Protein disulphide isomerase as a target for nanoparticle-mediated sensitisation of cancer cells to radiation. *Nanotechnology* **2016**, *27* (21).
46. Detappe, A.; Thomas, E.; Tibbitt, M. W.; Kunjachan, S.; Zavidij, O.; Parnandi, N.; Reznichenko, E.; Lux, F.; Tillemen, O.; Berbeco, R., Ultrasmall Silica-Based Bismuth Gadolinium Nanoparticles for Dual Magnetic Resonance-Computed Tomography Image Guided Radiation Therapy. *Nano Lett* **2017**, *17* (3), 1733-1740.
47. Li, N.; Yu, L. H.; Wang, J. B.; Gao, X. N.; Chen, Y. Y.; Pan, W.; Tang, B., A mitochondria-targeted nanoradiosensitizer activating reactive oxygen species burst for enhanced radiation therapy. *Chem Sci* **2018**, *9* (12), 3159-3164.
48. Nakayama, M.; Sasaki, R.; Ogino, C.; Tanaka, T.; Morita, K.; Umetsu, M.; Ohara, S.; Tan, Z. Q.; Nishimura, Y.; Akasaka, H.; Sato, K.; Numako, C.; Takami, S.; Kondo, A., Titanium peroxide nanoparticles enhanced cytotoxic effects of X-ray irradiation against pancreatic cancer model through reactive oxygen species generation in vitro and in vivo. *Radiation Oncology* **2016**, *11*.
49. Chithrani, D. B.; Jelveh, S.; Jalali, F.; van Prooijen, M.; Allen, C.; Bristow, R. G.; Hill, R. P.; Jaffray, D. A., Gold Nanoparticles as Radiation Sensitizers in Cancer Therapy. *Radiat Res* **2010**, *173* (6), 719-728.
50. Fang, X.; Wang, Y. L.; Ma, X. C.; Li, Y. Y.; Zhang, Z. L.; Xiao, Z. S.; Liu, L. J.; Gao, X. Y.; Liu, J., Mitochondria-targeting Au nanoclusters enhance radiosensitivity of cancer cells. *Journal of Materials Chemistry B* **2017**, *5* (22), 4190-4197.
51. Al Zaki, A.; Joh, D.; Cheng, Z. L.; De Barros, A. L. B.; Kao, G.; Dorsey, J.; Tsourkas, A., Gold-Loaded Polymeric Micelles for Computed Tomography-Guided Radiation Therapy Treatment and Radiosensitization. *ACS Nano* **2014**, *8* (1), 104-112.

52. Geng, F.; Song, K.; Xing, J. Z.; Yuan, C. Z.; Yan, S.; Yang, Q. F.; Chen, J.; Kong, B. H., Thio-glucose bound gold nanoparticles enhance radio-cytotoxic targeting of ovarian cancer. *Nanotechnology* **2011**, *22* (28), 285101.
53. Butterworth, K. T.; Coulter, J. A.; Jain, S.; Forker, J.; McMahon, S. J.; Schettino, G.; Prise, K. M.; Currell, F. J.; Hirst, D. G., Evaluation of cytotoxicity and radiation enhancement using 1.9 nm gold particles: potential application for cancer therapy. *Nanotechnology* **2010**, *21* (29), 295101.
54. Latimer, C. L. Octaarginine Labelled 30 nm Gold Nanoparticles as Agents for Enhanced Radiotherapy. University of Toronto, Toronto, 2013.
55. Kong, T.; Zeng, J.; Wang, X. P.; Yang, X. Y.; Yang, J.; McQuarrie, S.; McEwan, A.; Roa, W.; Chen, J.; Xing, J. Z., Enhancement of radiation cytotoxicity in breast-cancer cells by localized attachment of gold nanoparticles. *Small* **2008**, *4* (9), 1537-1543.
56. Janicke, R. U.; Sprengart, M. L.; Wati, M. R.; Porter, A. G., Caspase-3 is required for DNA fragmentation and morphological changes associated with apoptosis. *J Biol Chem* **1998**, *273* (16), 9357-9360.
57. Enns, L.; Bogen, K. T.; Wizniak, J.; Murtha, A. D.; Weinfeld, M., Low-dose radiation hypersensitivity is associated with p53-dependent apoptosis. *Mol Cancer Res* **2004**, *2* (10), 557-566.
58. Liu, Y.; Chen, W. Q.; Zhang, P. C.; Jin, X. D.; Liu, X. G.; Li, P.; Li, F. F.; Zhang, H. P.; Zou, G. Z.; Li, Q., Dynamically-enhanced retention of gold nanoclusters in HeLa cells following X-rays exposure: A cell cycle phase-dependent targeting approach. *Radiother Oncol* **2016**, *119* (3), 544-551.
59. Ojima, M.; Ban, N.; Kai, M., DNA double-strand breaks induced by very low X-ray doses are largely due to bystander effects. *Radiat Res* **2008**, *170* (3), 365-371.
60. Rosa, S.; Connolly, C.; Schettino, G.; Butterworth, K. T.; Prise, K., Biological mechanisms of gold nanoparticle radiosensitization. *Cancer Nano* **2017**, *8* (2), 1.
61. Ngwa, W.; Irabor, O. C.; Schoenfeld, J. D.; Hesser, J.; Demaria, S.; Formenti, S. C., Using immunotherapy to boost the abscopal effect. *Nat Rev Cancer* **2018**, *18* (5), 313-322.
62. Davidson, R. A.; Guo, T., Multiplication Algorithm for Combined Physical and Chemical Enhancement of X-ray Effect by Nanomaterials. *J Phys Chem C* **2015**, *119* (33), 19513-19519.
63. Peck, K. A.; Su, M. Q.; Lien, J.; Sharmah, A.; Guo, T., Sealable Spherical Mesoporous Silica Shell Nanoreactors as Fiducial Nanoscale Probes for X-rays. *J Phys Chem A* **2018**, *122* (43), 8686-8692.
64. Alizadeh, E.; Cloutier, P.; Hunting, D.; Sanche, L., Soft X-ray and Low Energy Electron-Induced Damage to DNA under N-2 and O-2 Atmospheres. *J Phys Chem B* **2011**, *115* (15), 4523-4531.
65. Chen, H. M.; Wang, G. D.; Chuang, Y. J.; Zhen, Z. P.; Chen, X. Y.; Biddinger, P.; Hao, Z. L.; Liu, F.; Shen, B. Z.; Pan, Z. W.; Xie, J., Nanoscintillator-Mediated X-ray Inducible Photodynamic Therapy for In Vivo Cancer Treatment. *Nano Lett* **2015**, *15* (4), 2249-2256.
66. Hildenbrand, G.; Metzler, P.; Pilarczyk, G.; Bobu, V.; Kriz, W.; Hosser, H.; Fleckenstein, J.; Krufczik, M.; Bestvater, F.; Wenz, F.; Hausmann, M., Dose enhancement effects of gold nanoparticles specifically targeting RNA in breast cancer cells. *Plos One* **2018**, *13* (1).
67. Hoertz, P. G.; Magnus-Aryitey, D.; Gupta, V.; Norton, C.; Doorn, S.; Ennis, T., Photocatalytic and radiocatalytic nanomaterials for the degradation of organic species. *Radiation Physics and Chemistry* **2013**, *84*, 51-58.



Three categories of enhancement acting on the damage of a segment of a nuclear DNA molecule in the cell